Journal of Power Sources 214 (2012) 314–318

Contents lists available at SciVerse ScienceDirect

Journal of Power Sources

journal homepage: www.elsevier.com/locate/jpowsour

Self-assembled synthesis of nanoflower-like $Li_4Ti_5O_{12}$ for ultrahigh rate lithium-ion batteries

Yu-Sheng Lin, Min-Chiao Tsai, Jenq-Gong Duh*

Department of Materials Science and Engineering, National Tsing Hua University, Hsinchu, Taiwan

HIGHLIGHTS

- The morphology reveals nanoflower-like shape with nanoplates crosslink.
- The thickness of $Li_4Ti_5O_{12}$ nanoplates was around 10 nm
- Nanoplates shorten lithium transportation path and facilitate rate capability.
- Nanoflower-like spinel lithium titanate shows an outstanding cycling behavior.

ARTICLE INFO

Article history:
Received 17 January 2012
Received in revised form
7 April 2012
Accepted 25 April 2012
Available online 4 May 2012

Keywords:
Lithium titanate
Hydrothermal
Nanoflower
High rate
Self-assembly

ABSTRACT

Nanoflower-like spinel lithium titanate is synthesized through combining sol/gel and hydrothermal process. The role of hydrothermally treating amorphous TiO_2 beads under the additive of LiOH precursor can derive nanocrystalline spinel lithium titanate with nanoflower-like shape. Afterward, calcination helps the formation of nanoflower-like spinel lithium titanate. The crystalline structure and morphological observation of the as-synthesized nanoflower-like $Li_4Ti_5O_{12}$ are characterized by X-ray diffraction (XRD) and scanning electron microscopy (SEM), respectively. The nanoflower-like structure can be revealed through the N_2 adsorption/desorption isotherm. It is demonstrated that the electrochemical performance is significantly improved by the architecture control. The nanoflower-like spinel lithium titanate shows outstanding cycling behavior of 148, 143, 141, 138, 133, 126, 118 mA h g^{-1} at 0.5, 1, 3, 5, 10, 20, 30 C, respectively. The reversible capacity at 30 C even remains over 80% of that at 0.5 C. The superior C-rate performance is associated with the nanoflower-like structure, facilitating lithium transportation ability during cycling. It is believed that the novel self-assembled synthesis for nanoflower-like lithium titantate can exhibit an excellent cycling performance and can be a good candidate for the next-generation anode material of ultrahigh rate Li-ion batteries for the application of electric vehicles.

1. Introduction

As energy storage devices, lithium-ion batteries are the dominant power source for portable consumer electronics, such as mobile phones and notebook computers. Besides, to meet the environmental concern for global issue, lithium-ion batteries have been used for electric vehicle and hybrid electric vehicle to save oil and to decrease exhaust emissions. The increasing demands for high-energy density and high-power density of batteries have attracted investigators to develop new materials for lithium-ion batteries. In present commercial lithium-ion batteries, graphite is a widely used as anode material [1]. However, graphite cannot satisfactorily meet the safety and rate performance requirements for future applications in EV and HEV. The theoretical capacity of graphite is only 372 mA h g^{-1}. Consequently, Sn-based materials have attracted particular interest as negative electrodes, due to their higher theoretical lithium storage capacities, higher lithium packing density and proper operating voltage [2]. Nevertheless, the most critical problem is the severe volume changes during lithium alloy and dealloy, causing electrode disintegration, reducing battery life, and finally limiting the possibility of commercialization [3,4].

Recently, spinel lithium titanate, $Li_4Ti_5O_{12}$, has attracted great interest as anode material for rechargeable lithium-ion batteries, due to its unique characteristics, including the zero-strain feature and the flat Li insertion voltage at about 1.55 V versus Li [5–7]. It is revealed that spinel host has an excellent structural stability and

* Corresponding author. Tel./fax: +886 3 5712686.
E-mail address: jgd@mx.nthu.edu.tw (J.-G. Duh).

0378-7753/$ – see front matter © 2012 Elsevier B.V. All rights reserved.
doi:10.1016/j.jpowsour.2012.04.072

a very small volume change during cycling. The space group of the spinel $Li_4Ti_5O_{12}$ is *Fd*3*m*. One part of lithium ions is located at (8a) sites, the other part of lithium ions and all titanium ions at (16d) sites, and oxygen ions at (32e) sites [8]. During cycling, 3 mol of lithium ions in tetrahedral sites (8a) are capable of inserting into the octahedral sites (16c) of $Li_4Ti_5O_{12}$ lattices, forming $Li_7Ti_5O_{12}$ rocksalt structure [7,9]. It accommodates Li-ions to have a theoretical capacity of 175 mA h g^{-1} with excellent cyclability and displays a discharge platform around 1.55 V vs. Li/Li^+, suppressing the reduction of electrolyte, thus reducing the impedance of cell and making batteries more safe. Nevertheless, $Li_4Ti_5O_{12}$ is a poor electrical conductor with a conductivity of only 10^{-13} S cm^{-1} at room temperature [10]. Currently, new strategy is to design porous spinel lithium titanate anode materials [11–17]. Accordingly, porous $Li_4Ti_5O_{12}$ anode materials give an ideal approach for the efficient transport of lithium ions at high cycling rates [11–17]. Thus, porous $Li_4Ti_5O_{12}$ is indeed a potential candidate material for high-rate lithium-ion batteries. Recently, mesoporous $Li_4Ti_5O_{12}$ has been synthesized via acidized carbon black as templates under hydrothermal condition [13]. It was demonstrated that the cycling stability could be significantly enhanced by mesoporous incorporation, especially at high cycling rate. Consequently, to further reduce the cost for fabrication without templates additive, the present work aims to develop a novel self-assembled synthesis for nanoflower-like spinel lithium titanate anode materials.

In general, spinel lithium titanate could be synthesized through solid-state reaction between lithium salts and titanium sources under high calcination temperature [18–20]. Various shapes of TiO_2 as titanium sources could be also reacted with lithium salts to obtain spinel lithium titanate. However, the final $Li_4Ti_5O_{12}$ hardly retained the original structure of TiO_2 precursors, owing to the high sintering temperature requirement for the formation of spinel $Li_4Ti_5O_{12}$, causing the grain coarsening and agglomeration of powders. One approach is to decrease the annealing temperature and time to alleviate the possibility of grain growth, possibly worsening the crystallinity of $Li_4Ti_5O_{12}$, even affecting the battery performance [20]. Hereafter, this study aims to develop newly self-assembled synthesis of spinel lithium titanate with crosslink of nanoplates, so-called nanoflower-like structure. This research tends to employ LiOH as starting material to obtain layered hydrous lithium titanate precursor under hydrothermal process without the formation of TiO_2, greatly reducing the calcination temperature without sacrificing the crystallinity [21]. According to the phase diagram between Li_2O and TiO_2, once TiO_2 is formed, it is necessary to obtain spinel lithium titanate by reacting with lithium salts at high temperature for a long time [22]. Consequently, nanoflower-like structure of spinel lithium titanate under the assistance of LiOH precursor could be successfully derived. It is predicted that the thickness of nanoplates in nanoflower-like structure is short enough to enable lithium ions to be penetrated even under ultra-high cycling rates, inspiring the novel anode materials for high-rate and high-power Li-ion batteries.

2. Experimental section

2.1. Material preparation

The chemicals used in the study were titanium(IV) isopropoxide (TTIP, 97%, Sigma–Aldrich), hexadecylamine (HDA, 90%, Sigma–Aldrich), absolute ethanol (99.5% Merck), lithium hydroxide (LiOH, Sigma–Aldrich). A general synthesis of amorphous TiO_2 submicron spheres was as follows. 1.58 g HDA was dissolved in 500 mL absolute ethanol. After dissolution, 20 mL TTIP was added under vigorous stirring at room temperature. The resulting white TiO_2 precipitation was aged at room temperature for 24 h, then TiO_2 beads were collected by centrifugation and washed with ethanol for at least three times, finally drying in air at room temperature.

In a typical synthesis of nanoflower-like $Li_4Ti_5O_{12}$, a stoichiometric amount of LiOH and as-synthesized TiO_2 submicron spheres (Li/Ti = 4:5) were mixed in 180 mL of ethanol solvent and stirred at room temperature, transferring to a Teflon-lined stainless steel autoclave (225 mL in volume) and then reacting in an air-flow electric oven at 180 °C for 6 h. After cooling down naturally, the precipitate was harvested by centrifugation and washed thoroughly with ethanol for at least three times. The products were further dried at 50 °C for 1 day. Eventually, the powder was calcined at 600 °C for 3 h to obtain nanoflower-like $Li_4Ti_5O_{12}$.

2.2. Materials characterization

The phase of as-synthesized powder was identified with an X-ray diffractometer (XRD, LabX XRD-6000, Shimadzu, Japan) operated at 30 kV and 20 mA using Cu Kα with a wavelength of 1.5406 Å. Morphological observation was carried out via field-emission scanning electron microscope (SEM; JSM-7600F, JEOL, Japan). The BET specific surface area was obtained from the N_2 adsorption/desorption isotherms at 77 K (Autosorb-1, Quantachrome).

2.3. Electrochemical measurement

Electrochemical tests were performed by using two-electrode of 2032 type coin cells (20 mm in diameter and 3.2 mm thick). The cells contained anode electrode, metallic lithium, polypropylene separator, and electrolyte of 1.0 M $LiPF_6$ in EC/DMC (1:1, vol.%), and were assembled in an argon glove box where both moisture and oxygen content were less than 1 ppm. The cells were cycled between 1 V and 2.5 V versus Li/Li^+. The C-rate capability test was performed at the charge/discharge rate of 0.5, 1, 3, 5, 10, 20, and 30 C. The electrochemical impedance spectroscopy (EIS) measurements were carried out with a potentiostat (PAR model 263A, EG&G). The sinusoidal excitation voltage applied to the cells was 10 mV rms with a frequency range of between 100 kHz and 10 mHz.

3. Results and discussion

Fig. 1 shows the X-ray diffraction (XRD) pattern of powders after hydrothermal process and calcination. The structure of the products after hydrothermal process is close to layered hydrous lithium titanate with a C-based centered orthorhombic structure (JCPDS Card No. 47-0123). It was worth noting that the peak at ~10.5° indicated the layered structure. After calcination, all the diffraction peaks can be indexed on the basis of a cubic spinel lithium titanate, $Li_4Ti_5O_{12}$ (JCPDS Card No. 26-1198). That is to say, the layered hydrous lithium titanate was completely converted to spinel $Li_4Ti_5O_{12}$ without the presence of impurity. It was revealed that high purity $Li_4Ti_5O_{12}$ could be prepared by calcinating layered hydrous lithium titanate precursors under relatively low temperature, say, 600 °C. Furthermore, no impurity could be detected through X-ray diffraction pattern of spinel lithium titanate. It was demonstrated that the self-assembled synthesis of spinel lithium titanate did not cause the impurity.

The SEM images of amorphous TiO_2 submicron spheres, layered hydrous lithium titanate after hydrothermal process, and spinel lithium titanate after calcination are revealed in Fig. 2. The SEM image of amorphous TiO_2 precursors is shown in Fig. 2a. The diameter of monodispersed TiO_2 precursors was around 400 nm with smooth surface. With the addition of HDA as a structure-directing agent, the solvation force between nanoclusters strengthened the formation of amorphous TiO_2 spheres. Besides, the agglomeration of TiO_2 beads could be avoided by the HDA

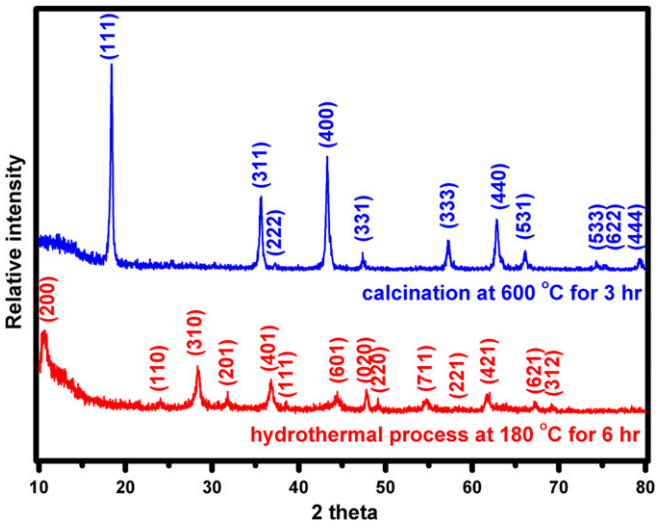

Fig. 1. The XRD patterns of powders after hydrothermal process and calcination.

additive. Fig. 2b shows the SEM image of layered hydrous lithium titanate after hydrothermal process. The morphology reveals the crosslink of nanoplates, designating nanoflower-like shape of layered hydrous lithium titanate. The thickness of nanoplates was around 10 nm. The connections between these nanoplates promoted large pore volume in the powders. In general, the nanoplates structure is associated with the layered structure of hydrous lithium titanate after hydrothermal process. Layered structure is originated from the insertion of metal ions or organic species [23–25]. In this study, nanoflower-like structure might be related to the insertion of Li^+ ions between layers consisted of TiO_6 octahedrons under hydrothermal process with LiOH as precursors, inducing anisotropic growth, further generating nanoplates structure. Besides, the shape of spinel lithium titanate after calcination at 600 °C is observed in Fig. 2c. It was demonstrated that the appearance of spinel lithium titanate remained after calcination. The grain growth and agglomeration of powder were even restricted, due to the relatively low calcination temperature by using LiOH as precursors.

From the view of morphological observations in SEM images, nanoflower-like structure could be naturally obtained by self-assembled synthesis. Nevertheless, the overall evidence of nanoflower-like architecture was also required. N_2 adsorption/desorption analysis was used to examine the structure of spinel lithium titanate. The N_2 adsorption/desorption curve of nanoflower-like $Li_4Ti_5O_{12}$ was revealed in Fig. 3. There is a hysteresis loop in the nitrogen adsorption/desorption isotherms at relative pressures of $P/P_o = 0.85–0.97$, implying the filling of the porous framework [26]. The nitrogen adsorption/desorption curve of nanoflower-like $Li_4Ti_5O_{12}$ exhibits a typical type IV isotherm and a type H3 hysteresis loop. Characteristic features of the type IV isotherm are its hysteresis loop, associated with capillary force taking place in the pores. Besides, the type H3 hysteresis loop is observed between nanoplate-like particles, giving rise to slit-shaped pores, matching the morphological observation in Fig. 2c. The corresponding specific surface area and pore volume were 40.2 $m^2\ g^{-1}$ and 0.184 cc g^{-1}, respectively. It was speculated that the increase in pore volume is related to crosslink between nanoplates, facilitating lithium transportation during cycling.

Fig. 4 illustrates the C-rate capability of nanoflower-like spinel lithium titanate anode materials. The 1st capacity of $Li_4Ti_5O_{12}$ nanoflowers at 0.5 C was ~148 mA h g^{-1}. Afterward, the lithium insertion and extraction rates increased stepwise up to 30 C. The capacity of $Li_4Ti_5O_{12}$ nanoflowers at the current rate of 1, 3, 5, 10, 20, 30 C was around 143, 141, 138, 133, 126, 118 mA h g^{-1}, respectively. As the current rate decreased to 0.5 C again, the capacity remained around 145 mA h g^{-1} without any decay in the following 60 cycles. Consequently, the nanoflower-like $Li_4Ti_5O_{12}$ anode material exhibits an outstanding performance at rate capability test. It should be noted that the cycling stability under high current rates was significantly affected by the architectural control. Herein, the nanoflower-like $Li_4Ti_5O_{12}$ delivered a better cycling performance, owing to its shorter lithium diffusion route along thin nanoplates.

The relationship between capacity and retention versus current rate of nanoflower-like $Li_4Ti_5O_{12}$ is described in Fig. 5. The thickness of nanoplates in the nanoflower-like $Li_4Ti_5O_{12}$ anode materials was thin enough to permit lithium ions and electrons to be completely combined even at a sudden time. Thus, the nanoflower-like spinel lithium titanate could endure ultrahigh cycling rates, such as 30 C. From the rate capability relationship, the capacity of nanoflower-like $Li_4Ti_5O_{12}$ at 1, 3, 5, 10, 20, 30 C retained 97, 95, 93, 90, 85, 80% of cell capacity at 0.5 C. It is apparent that the cycling stability at high rate is strongly associated with the structure of spinel lithium titanate. Furthermore, spinel lithium titanate with nanoflower-like structure could tolerate high current rates.

Fig. 6 displays the charge/discharge curves of nanoflower-like $Li_4Ti_5O_{12}$ under various cycling rates. All curves were selected during the last cycle under different current rates. It was demonstrated that the nanoflower-like material could sustain excellent charge and discharge rates. The charge/discharge curves of nanoflower-like $Li_4Ti_5O_{12}$ were nearly identical at 0.5 C and 1 C, as shown in Fig. 6. Then, the discharge voltage decreased with increasing current density. The discharge voltage plateaus at 0.5, 1, 3, 5, 10, 20, 30 C were around 1.55, 1.55, 1.53, 1.50, 1.47, 1.40, 1.34 V. The voltage plateaus during lithium insertion process were nearly identical, as the current rate was below 5 C. Consequently, the polarization phenomenon was not severe for high rate cycling measurement. Additionally, the voltage plateaus were clearly

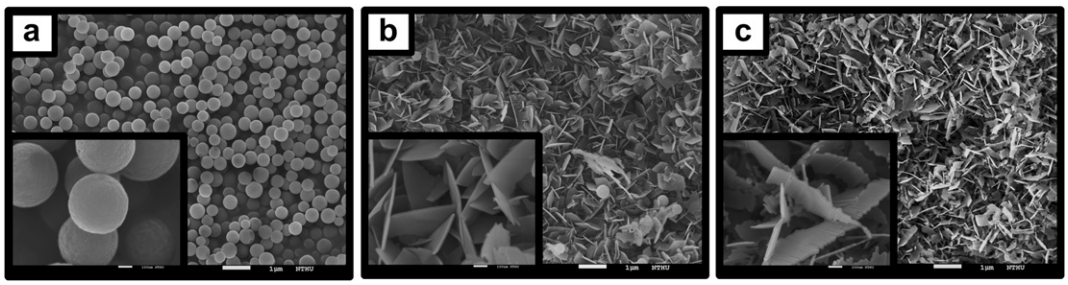

Fig. 2. The SEM images of (a) amorphous TiO_2 submicron spheres by sol/gel method, (b) layered hydrous lithium titantate after hydrothermal process, and (c) nanoflower-like spinel lithium titanate after calcination.

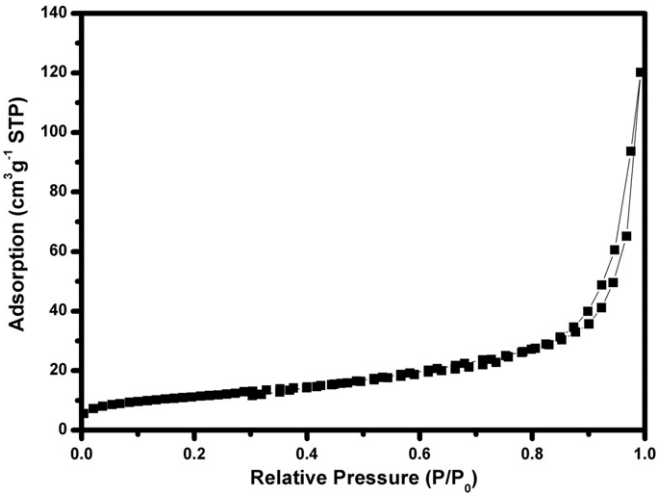

Fig. 3. The nitrogen adsorption/desorption isotherm of nanoflower-like spinel lithium titanate.

visible even at 30 C, indicating a good lithiation/delithiation process at such short reaction time. Herein, nanoflower-like spinel lithium titanate anode materials indeed retained outstanding rate capability.

In order to demonstrate the excellent rate capability and cycling stability, long cycling tests of nanoflower-like lithium titantate anodes under 1, 5, 30 C were examined in Fig. 7. The initial capacity of nanoflower-like $Li_4Ti_5O_{12}$ at 1, 5, 30 C was relatively lower than the capacity showed in Fig. 4, especially at 5 C and 30 C. It might be due to the wettability between electrolyte and electrodes. The capacity of cell increased gradually to a stable value after a few cycles. The maximum capacity of nanoflower-like $Li_4Ti_5O_{12}$ at 1, 5, 30 C was around 144, 141, 125 mA h g^{-1}, respectively. The 300th capacity of nanoflower-like $Li_4Ti_5O_{12}$ at 1, 5, 30 C was around 136, 133, 111 mA h g^{-1}, respectively. Then, the retention of nanoflower-like $Li_4Ti_5O_{12}$ was around 94, 94, 89%, respectively, at 1, 5, 30 C. As the current rate increased to 30 C, the capacity of 125 mA h g^{-1} could be achieved, indicating that over 86% lithium ions at 0.5 C could be reversibly inserted and extracted within 2 min. Besides, the retention of $Li_4Ti_5O_{12}$ nanoflowers retained higher than 89%

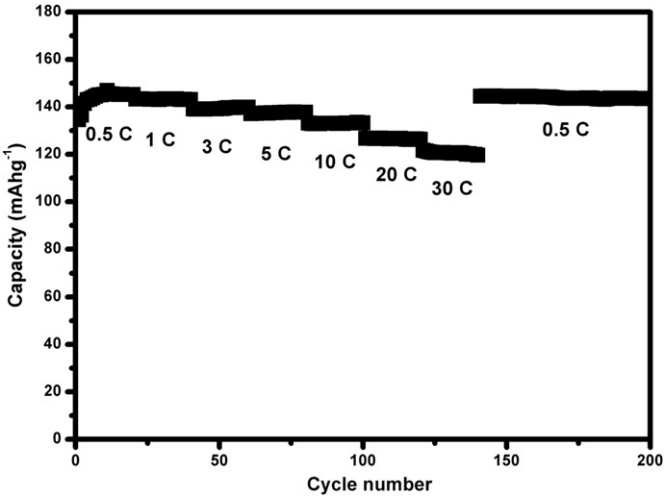

Fig. 4. The rate capability measurement of nanoflower-like spinel lithium titanate at various cycling rates of 0.5, 1, 3, 5, 10, 20, 30 C.

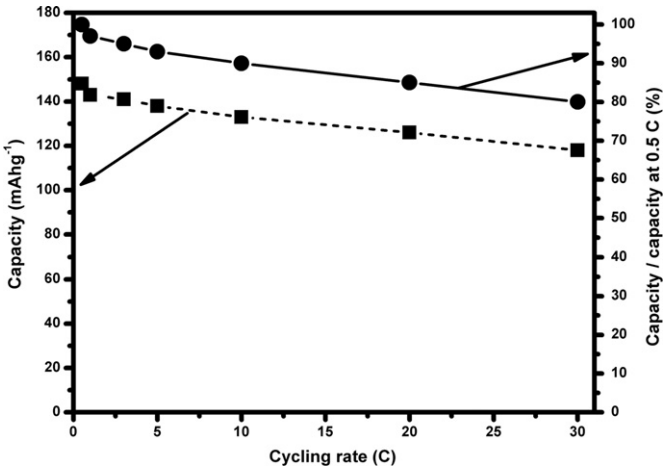

Fig. 5. The relationship of reversible capacity and capacity ratio versus cycling rates of nanoflower-like spinel lithium titanate anode material.

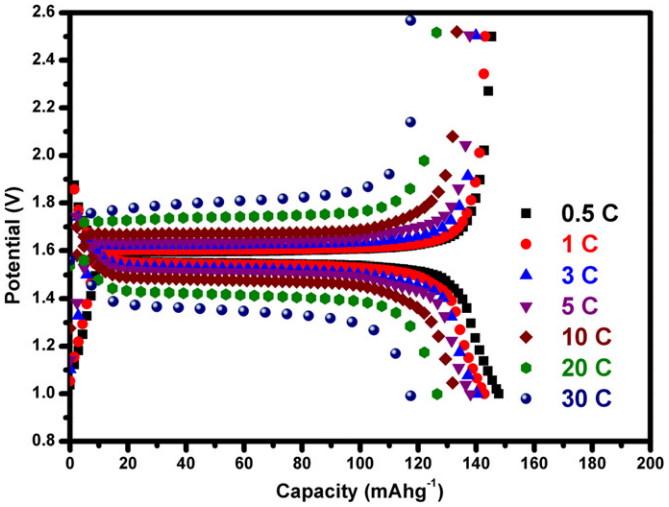

Fig. 6. The charge/discharge curves of nanoflower-like spinel lithium titanate at various cycling rates of 0.5, 1, 3, 5, 10, 20, 30 C.

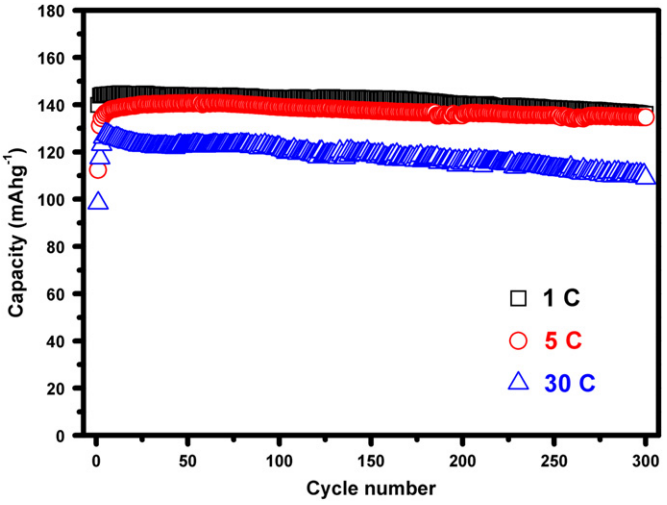

Fig. 7. The cycling stability measurements for long cycles of nanoflower-like spinel lithium titanate at 1, 5, 30 C.

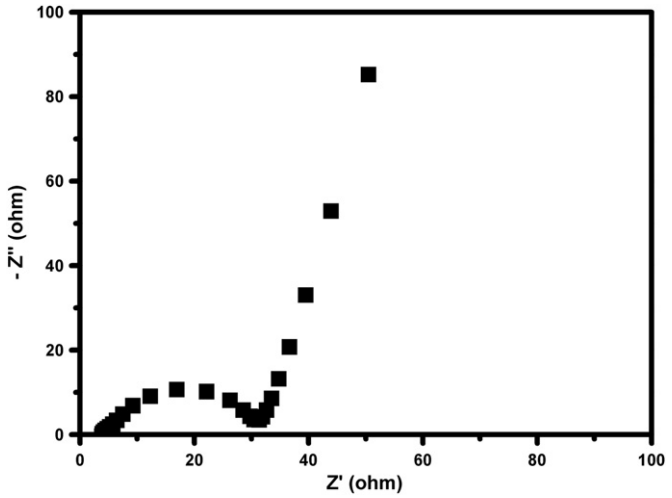

Fig. 8. The electrochemical impedance spectroscopy of spinel lithium titanate nanoflowers.

after 300 cycles, displaying a high structural stability of nanoflower shape. As a result, nanoflower-like spinel lithium titanate by self-assembled synthesis exhibited an outstanding cycling performance.

To figure out the effect on rate capability, electrochemical impedance spectroscopy (EIS) measurement is carried out in Fig. 8. An intercept at the Z' axis in high frequency was attributed to the ohmic resistance (R_e), representing the resistance of the electrolyte. The semicircle in the middle frequency range was associated with the charge transfer resistance (R_{ct}). It was revealed that the R_e was $\sim$5 Ω and the R_{ct} was $\sim$25 Ω. The value of R_{ct} is small enough to force lithium ions and electrons to be reacted immediately, accelerating the transportation of lithium ions and electrons. As a result, $Li_4Ti_5O_{12}$ nanoflower anodes could display an outstanding rate capability and an excellent cycling stability.

4. Conclusion

Nanoflower-like spinel lithium titanate is synthesized through integrating sol/gel and hydrothermal process. Crosslink of $Li_4Ti_5O_{12}$ nanoplates could be revealed in the as-synthesized spinel $Li_4Ti_5O_{12}$ powder. The thickness of $Li_4Ti_5O_{12}$ nanoplates was $\sim$10 nm, shortening the lithium transportation path and facilitating rate capability. The capacity of spinel $Li_4Ti_5O_{12}$ nanoflowers at the current rate of 0.5, 1, 3, 5, 10, 20, 30 C was around 148, 143, 141, 138, 133, 126, 118 mA h g^{-1}, respectively. At ultrahigh C-rate test for long cycles, the capacity remained 125 mA h g^{-1} at 30 C and retained over 89% after 300 cycles, manifesting a superior cycling performance. It is demonstrated that the nanoflower-like spinel lithium titanate might be a promising anode material as high-performance anodes for next-generation LIBs.

Acknowledgments

The authors would like to thank the GREEN ENERGY ELECTRODE, INC and National Science Council, Taiwan under Contract No. 97-2221-E-007-021-MY3 for financial support. The authors also thank the Material and Chemical Research Lab, Industrial Technology Research Institute, Taiwan for the assistance of cell assembly.

References

[1] Y.S. Lin, J.G. Duh, H.S. Sheu, J. Alloys Compd. 509 (2011) 123–127.
[2] M. Winter, J.O. Besenhard, Electrochim. Acta 45 (1999) 31–50.
[3] Y.S. Lin, J.G. Duh, D.T. Shieh, M.H. Yang, J. Alloys Compd. 490 (2010) 393–398.
[4] Y.S. Lin, J.G. Duh, M.H. Hung, J. Phys. Chem. C 114 (2010) 13136–13141.
[5] T. Ohzuku, A. Ueda, N. Yamamoto, J. Electrochem. Soc. 142 (1995) 1431–1435.
[6] L. Kavan, J. Prochazka, T.M. Spitler, M. Kalbac, M. Zukalova, T. Drezen, M. Gratzel, J. Electrochem. Soc. 150 (2003) A1000–A1007.
[7] L. Kavan, M. Gratzel, Electrochem. Solid-State Lett. 5 (2002) A39–A42.
[8] H. Ge, N. Li, D. Li, C. Dai, D. Wang, J. Phys. Chem. C 113 (2009) 6324–6326.
[9] C.T. Hsieh, J.Y. Lin, J. Alloys Compd. 506 (2010) 231–236.
[10] P.P. Prosini, R. Mancini, L. Petrucci, V. Contini, P. Villano, Solid State Ionics 144 (2001) 185–192.
[11] N. He, B. Wang, J. Huang, J. Solid State Electrochem. 14 (2010) 1241–1246.
[12] C. Jiang, Y. Zhou, I. Honma, T. Kudo, H. Zhou, J. Power Sources 166 (2007) 514–518.
[13] Y.S. Lin, J.G. Duh, J. Power Sources 196 (2011) 10698–10703.
[14] L. Shen, C. Yuan, H. Luo, X. Zhang, K. Xu, Y. Xia, J. Mater. Chem. 20 (2010) 6998–7004.
[15] E.M. Sorensen, S.J. Barry, H.K. Jung, J.R. Rondinelli, J.T. Vaughey, K.R. Poeppelmeier, Chem. Mater. 18 (2006) 482–489.
[16] S.W. Woo, K. Dokko, K. Kanamura, Electrochim. Acta 53 (2007) 79–82.
[17] Y. Tang, L. Yang, S. Fang, Z. Qiu, Electrochim. Acta 54 (2009) 6244–6249.
[18] T. Yuan, R. Cai, R. Ran, Y. Zhou, Z. Shao, J. Alloys Compd. 505 (2010) 367–373.
[19] T. Yuan, R. Cai, P. Gu, Z. Shao, J. Power Sources 195 (2010) 2883–2887.
[20] L. Cheng, J. Yan, G.N. Zhu, J.Y. Luo, C.X. Wang, Y.Y. Xia, J. Mater. Chem. 20 (2010) 595–602.
[21] M. Sugita, M. Tsuji, M. Abe, Bull. Chem. Soc. Jpn. 63 (1990) 1978–1984.
[22] G. Izquierdo, A.R. West, Mater. Res. Bull. 15 (1980) 1655–1660.
[23] P.C. Chen, M.C. Tsai, H.C. Chen, I.N. Lin, H.S. Sheu, Y.S. Lin, J.G. Duh, H.T. Chiu, C.Y. Lee, J. Mater. Chem. 22 (2012) 5349–5355.
[24] M.C. Tsai, J.C. Chang, H.S. Sheu, H.T. Chiu, C.Y. Lee, Chem. Mater. 21 (2009) 499–505.
[25] J. Huang, Y. Cao, Z. Deng, H. Tong, J. Solid State Chem. 184 (2011) 712–719.
[26] K.S.W. Sing, Pure Appl. Chem. 54 (1982) 2201–2218.